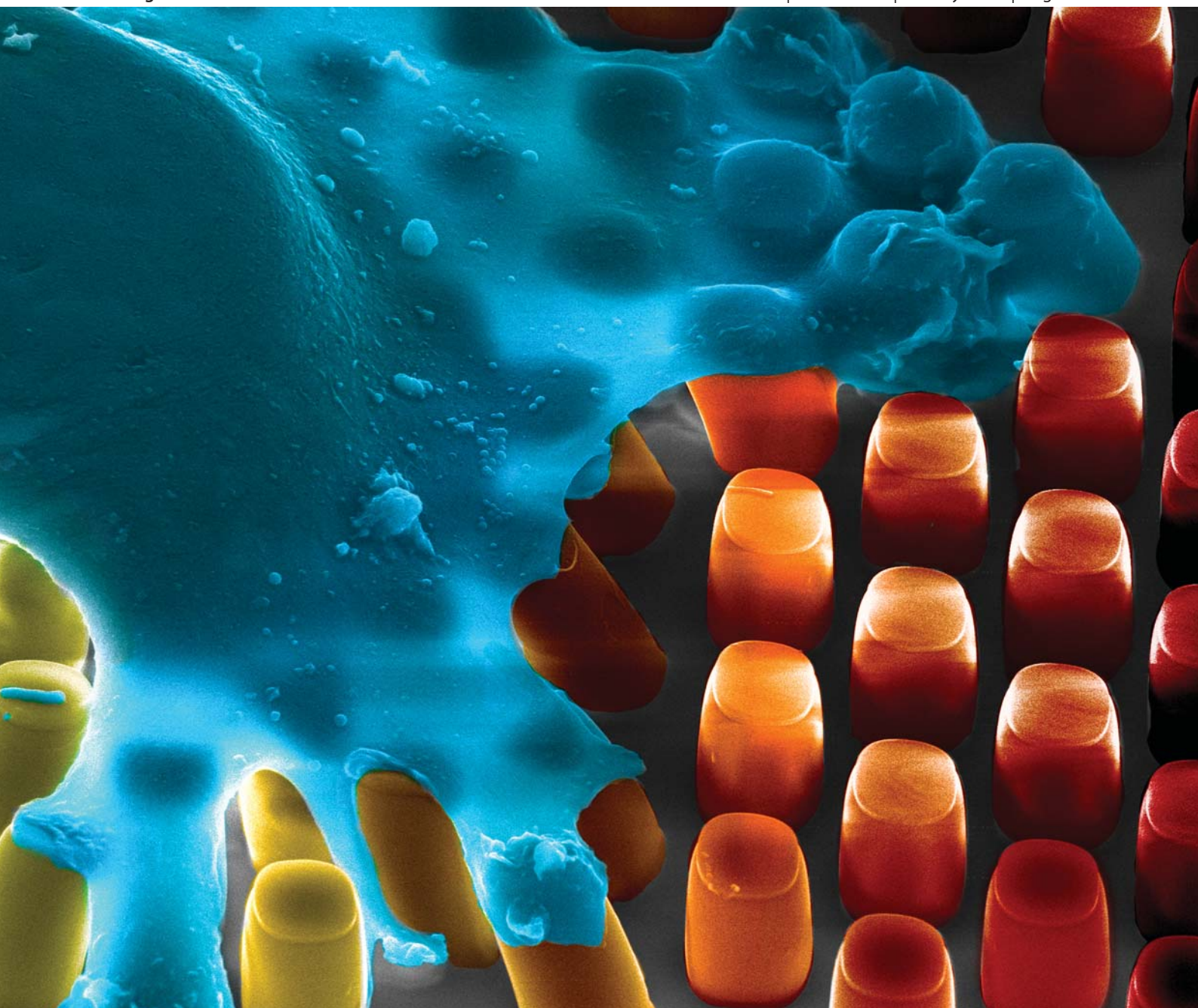


# Soft Matter

[www.rsc.org/softmatter](http://www.rsc.org/softmatter)

Volume 7 | Number 10 | 21 May 2011 | Pages 4517–5048



ISSN 1744-683X

RSC Publishing

**COMMUNICATION**

Ryan D. Sochol *et al.*  
Unidirectional mechanical cellular stimuli *via* micropost array  
gradients

Cite this: *Soft Matter*, 2011, **7**, 4606

www.rsc.org/softmatter

## Unidirectional mechanical cellular stimuli *via* micropost array gradients†

Ryan D. Sochol,<sup>\*a</sup> Adrienne T. Higa,<sup>a</sup> Randall R. R. Janairo,<sup>b</sup> Song Li<sup>b</sup> and Liwei Lin<sup>a</sup>

Received 31st January 2011, Accepted 9th March 2011

DOI: 10.1039/c1sm05163f

**Diverse cellular processes are influenced by the mechanical properties of the substrate. Here we introduce the methodology of constructing micropost array gradients to investigate the effects of unidirectional substrate stiffness cues on living cells. Experimental results revealed preferential cell migration in the direction of increasing micropost stiffness.**

A wide range of biological processes, such as angiogenesis, immune response, and wound repair, rely strongly on environmental stimuli.<sup>1</sup> Elucidating the cellular response to various external cues enables researchers to better predict and control cellular behavior—a necessity for biological applications including tissue engineering, biomaterials, and regenerative medicine.<sup>2</sup> It has been demonstrated that cellular functions are influenced by a variety of microenvironmental cues, such as chemical<sup>3</sup> and mechanical<sup>4</sup> signals. Recent work has revealed significant roles of mechanical cues for living cells. Researchers have shown that substrate-based mechanical stimuli influence diverse cellular processes, such as focal adhesion development,<sup>5</sup> directional migration (*i.e. via* durotaxis),<sup>6</sup> and stem cell lineage specification.<sup>7,8</sup> In order to study the cellular response to substrates of varying rigidity, researchers have employed hydrogel photopolymerization-based methods to fabricate substrates with either a low number<sup>9,10</sup> or high number<sup>11,12</sup> of substrate stiffnesses. Micromachining methods can potentially provide advantages for studying the cellular response to substrate-based biophysical stimuli by enabling simplified fabrication processes, enhanced user control over substrate stiffness and improved device repeatability. Here, the technique of using micromachining processes to construct micropost array gradients with varying stiffnesses is proposed to investigate the cellular response to substrate-based mechanical cues.

Methods for engineering substrates with microtopography (*e.g.*, microgrooves or microposts) facilitate simple microfabrication, accurate feature definition, and high repeatability.<sup>13–15</sup> Previously, micropost arrays have been used to detect cellular traction forces on the substrate by modeling each micropost as a cantilever.<sup>14,15</sup> One

report has demonstrated the use of identical elliptical microposts for applying bidirectional stiffness cues to cells.<sup>13</sup> In this work, microposts of varying radii, and thus varying stiffnesses, were employed to apply unidirectional mechanical cues to living cells. Micropost array stiffness gradients with low gradient strength ( $\mu\text{SG}_L$ ) and high gradient strength ( $\mu\text{SG}_H$ ) were constructed to examine the effects of unidirectional biophysical stimuli on the motility of bovine aortic endothelial cells (BAECs).

Fig. 1a illustrates the micropost array gradient concept. In contrast to prior reports of microposts with uniform radii<sup>14,15</sup> or identical shapes,<sup>13</sup> for this study, the radii of arrayed microposts (Fig. 1a, '*r*') were increased in a single direction. A constant interpost spacing (Fig. 1a, '*T*') of 2  $\mu\text{m}$  was designed along the axis of increasing micropost radii. Fig. 1b illustrates the deformation of a micropost in response to a force applied at the top of the micropost and the theoretical formula used to calculate micropost stiffness.<sup>16</sup> The stiffness of a micropost can be geometrically tuned by adjusting either the height or radius of the micropost. For fabricating gradients of micropost stiffness, modulating micropost radii while maintaining a uniform structural height facilitates simple fabrication *via* one-mask soft lithography processes. Thus, the heights of the microposts were kept constant at 7  $\mu\text{m}$  while the radii of the microposts increased.

Two types of micropost array stiffness gradients were designed corresponding to: (i) low gradient strength ( $\mu\text{SG}_L$ ), and (ii) high gradient strength ( $\mu\text{SG}_H$ ). Both substrate areas were approximately  $500 \times 500 \mu\text{m}^2$ , consisting of thousands of microposts. Micropost radii were increased continuously over the course of the substrates, corresponding to post-to-post stiffness increments of  $0.5 \text{ nN } \mu\text{m}^{-1}$  and  $7.5 \text{ nN } \mu\text{m}^{-1}$  for the  $\mu\text{SG}_L$  and the  $\mu\text{SG}_H$ , respectively (Fig. 1c). The  $\mu\text{SG}_L$  included radii ranging from 1 to 2  $\mu\text{m}$ , corresponding to physiologically relevant stiffnesses of 5 to  $50 \text{ nN } \mu\text{m}^{-1}$ .<sup>15</sup> The  $\mu\text{SG}_H$  included radii ranging from 1 to 3  $\mu\text{m}$ , corresponding to micropost stiffnesses of approximately 5 to  $390 \text{ nN } \mu\text{m}^{-1}$ . When seeded cells spread on the micropost array gradients, they interact with microposts that increase in stiffness in a single, designed direction. For example, Fig. 1d shows a false-colored SEM image of a BAEC spread over microposts that include 28 distinct stiffness values, with micropost stiffness increasing from post-to-post rightward (*yellow to red*).

Micropost array gradient fabrication and preparation are discussed in the ESI†. Briefly, the micropost array gradients were fabricated *via* standard soft lithography processes. To improve cellular attachment to the top surfaces of the microposts, the substrates were selectively microcontact-printed with the protein, fibronectin, *via* previously described processes.<sup>14</sup> To preclude the

<sup>a</sup>Berkeley Sensor and Actuator Center, Department of Mechanical Engineering, University of California, Berkeley, 668 Sutardja Dai Hall, Berkeley, CA, 94720, USA. E-mail: rsochol@gmail.com

<sup>b</sup>Department of Bioengineering, University of California, Berkeley, and UC Berkeley-UCSF Bioengineering Graduate Program, CA, 94720, USA

† Electronic supplementary information (ESI) available: Micropost array gradient fabrication and preparation. See DOI: 10.1039/c1sm05163f

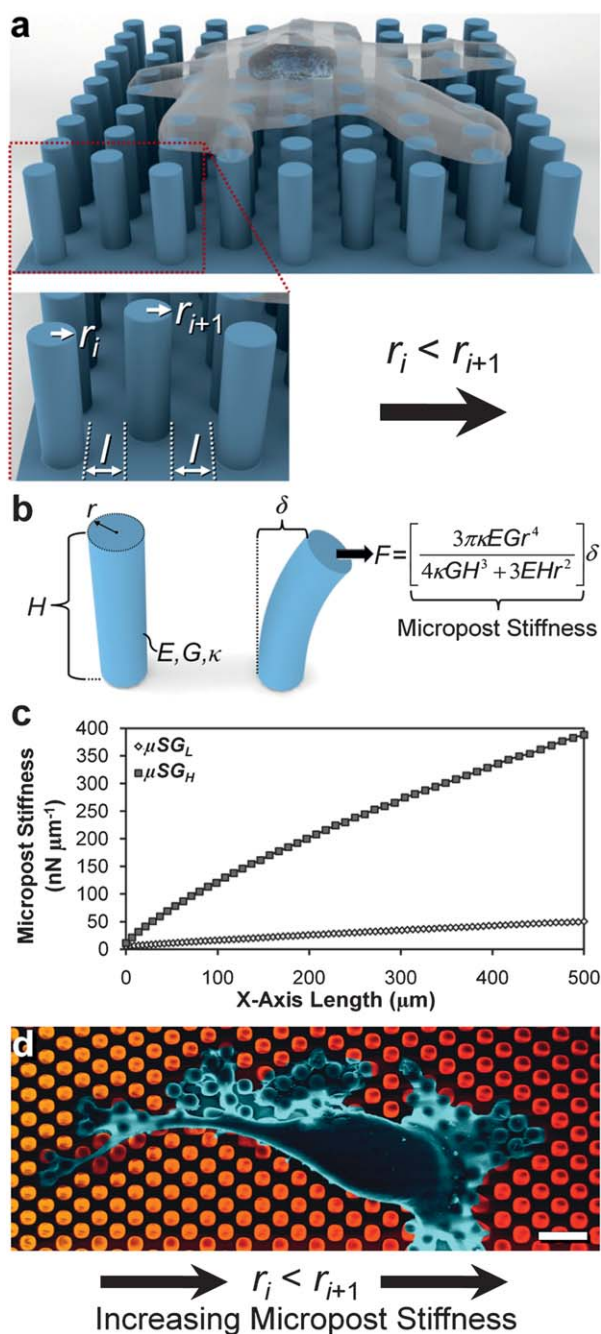


**Fig. 1** Micropost array stiffness gradients. (a) Conceptual illustration of a cell seeded on a microtopographic stiffness gradient with an enlarged view of individual microposts with increasing radii ( $r$ ) and equivalent interpost spacing ( $I$ ). (b) Micropost cantilever model. The linear stiffness at the top of the micropost is derived from its geometric and material properties, including the Young's modulus ( $E$ ), shear modulus ( $G$ ), shear coefficient ( $\kappa$ ), micropost height ( $H$ ), and micropost radius ( $r$ ). A force applied at the top of the micropost ( $F$ ), parallel to the substrate, will result in a displacement at the top of the micropost ( $\delta$ ). (c) Micropost stiffness over the length of the micropost array stiffness gradient with low gradient strength ( $\mu\text{SG}_L$ ) and high gradient strength ( $\mu\text{SG}_H$ ). (d) False-colored SEM image of a bovine aortic endothelial cell (BAEC) (*blue*) seeded on a micropost array stiffness gradient with microposts increasing in stiffness (*yellow to red*). Scale bar = 10  $\mu\text{m}$ .

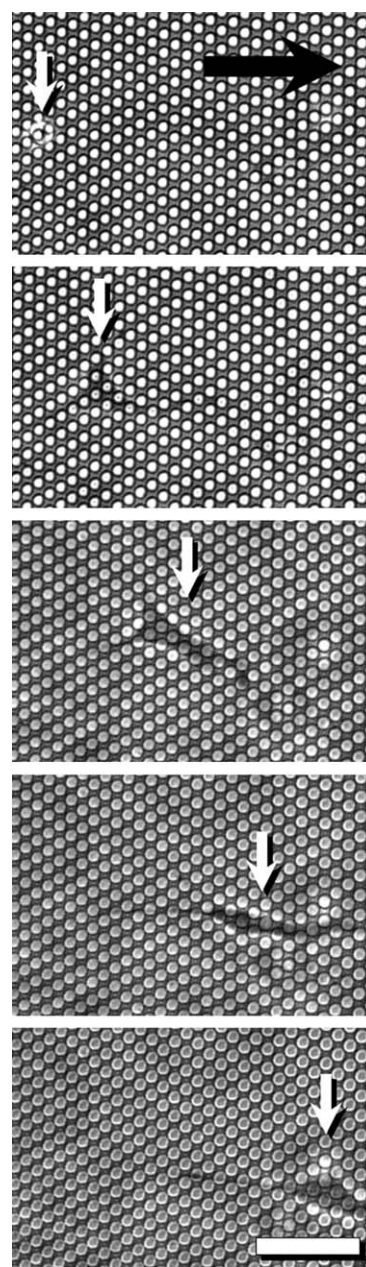


**Fig. 2** Cell migration on a micropost array stiffness gradient. Sequential time-lapse images of a BAEC (*white arrows*) migrating in the direction of increasing micropost stiffness (*black arrow*). Scale bar = 50  $\mu\text{m}$ .

potential effects of substrate-immobilized chemical gradients<sup>17</sup> and variable surface densities of topography,<sup>18,19</sup> the area surrounding individual microposts was modulated to maintain a consistent percentage of extracellular matrix protein coverage (%ECM) and topographic surface area for regimes of different micropost radii. Specifically, while the interpost spacing along the axis of increasing stiffness was held constant at 2  $\mu\text{m}$ , the interpost spacing perpendicular to the axis of increasing stiffness was adjusted to compensate for changes in micropost radii such that:

$$\%ECM = \frac{\pi r^2}{(2r+s)(2r+I)} = \text{Constant} \quad (1)$$

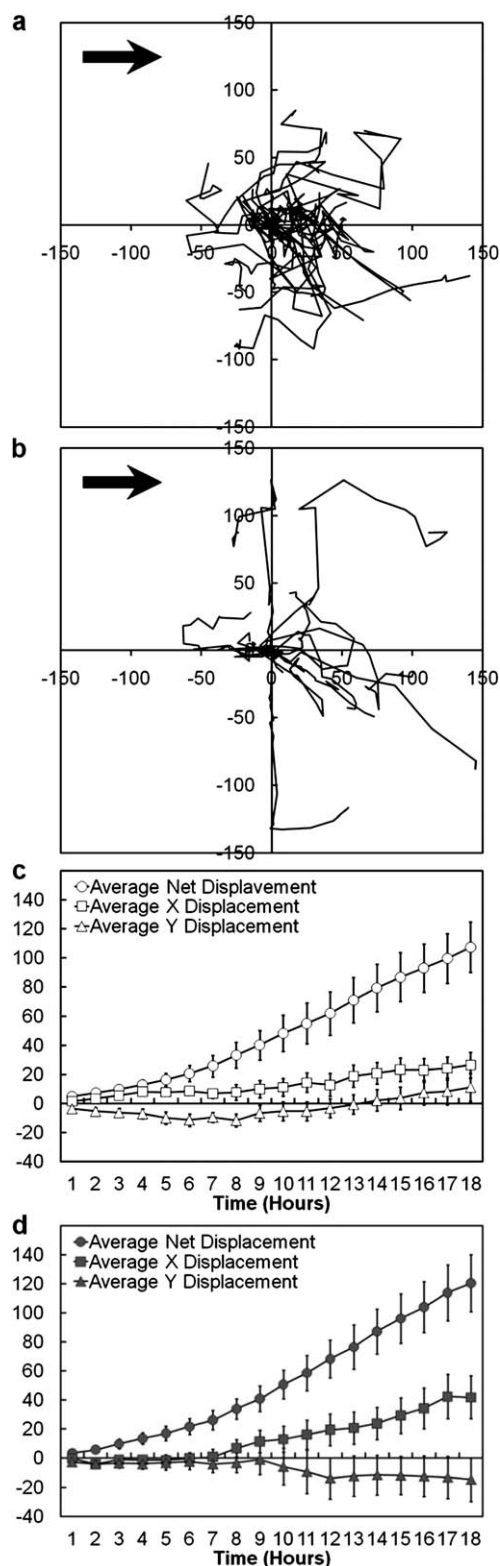


**Fig. 3** Experimental results of BAEC migration on micropost array stiffness gradients for 18 hour studies. Cell paths for (a) 23 cells seeded on the  $\mu\text{SG}_L$  and (b) 13 cells seeded on the  $\mu\text{SG}_H$ . Axis units =  $\mu\text{m}$ ; black arrows denote the direction of increasing micropost stiffness. Averaged cell displacements *versus* time for BAECs seeded on the (c)  $\mu\text{SG}_L$  (white) and (d)  $\mu\text{SG}_H$  (dark grey). Error bars denote s.e.m.

where  $r$  is the micropost radius,  $s$  is the spacing between microposts perpendicular to the axis of increasing stiffness and  $l$  is the interpost spacing parallel to the axis of increasing stiffness. Both the  $\mu\text{SG}_L$  and the  $\mu\text{SG}_H$  included equivalent %ECM and topographic surface densities of 20% to maintain consistency between the two gradients.

BAECs were seeded onto the micropost array gradients to study the effects of the substrates on cellular migration. Time-lapse videos of cell movement on both micropost array gradients were generated in parallel from phase contrast microscopic images taken over the course of 18 hour studies. Because cell–cell interactions can affect directional migration, data were collected from single cells with only substrate contact. Cell area centroids were tracked during the studies to quantify the directional response of BAECs seeded on each microtopographic gradient. A previously developed tactic index (TI) was employed to quantitatively evaluate the bias of cell migration in the direction of the migratory cues.<sup>11,20</sup> Due to the time-length of the study, the average TI was approximated as:

$$\text{TI} = \frac{X}{L} \quad (2)$$

where  $X$  and  $L$  are the mean displacement in the gradient direction and total path length, respectively.<sup>11</sup> Thus, a TI of 0 indicates unbiased movement, while a TI of 1 indicates fully biased movement in the direction of the mechanical stimuli.

The  $p$  values for this study were calculated *via* unpaired Student's  $t$  tests. Differences with a  $p$  value less than 0.05 were considered statistically significant. The experimental results are presented as mean  $\pm$  standard error of the mean (s.e.m.).

Experimental observations revealed that both micropost array stiffness gradients influenced directional motility, as seeded BAECs migrated preferentially in the direction of increasing micropost stiffness. Fig. 2 shows sequential time-lapse images of a BAEC (white arrows) migrating in the direction of increasing micropost stiffness (black arrow) on the  $\mu\text{SG}_L$ . The two-dimensional 18 hour cell paths for migration on the  $\mu\text{SG}_L$  and  $\mu\text{SG}_H$  are shown in Fig. 3a and b, respectively. On the  $\mu\text{SG}_L$ , seeded BAECs were found to displace an average of  $26.5 \pm 8.7 \mu\text{m}$  ( $n = 23$  cells) in the direction of increasing micropost stiffness by the end of the 18 hour studies (Fig. 3c). The maximum observed displacements during the studies were  $141 \mu\text{m}$  for cell movement in the direction of increasing micropost stiffness and  $45 \mu\text{m}$  for displacement opposite to that direction. At the end of the studies, 70% (16 from a total of 23) of BAECs exhibited displacement in the direction of increasing stiffness relative to their initial positions at the start of the study. Higher gradient strength was found to enhance the directional response. Cells on the  $\mu\text{SG}_H$  exhibited an average final displacement of  $41.9 \pm 14.7 \mu\text{m}$  in the direction of increasing micropost stiffness (Fig. 3d), with maximum observed displacements of  $145 \mu\text{m}$  for movement in the direction of increasing stiffness and  $24 \mu\text{m}$  for displacement opposite to that direction. By the end of the 18 hour studies, the percentage of cells that exhibited displacement in the direction of increasing micropost stiffness increased to 77% (10 from a total of 13 cells). These results are consistent with past studies of the cellular response to substrate stiffness cues.<sup>6,11,12</sup> Similar to prior work, increased gradient strength was found to enhance cell migration in the direction of increasing substrate stiffness.<sup>11</sup>

The average TI on the  $\mu\text{SG}_L$  was  $0.246 \pm 0.083$ , which indicates biased movement in the direction of increasing micropost stiffness. The average TI for BAEC movement on the  $\mu\text{SG}_H$  increased to

$0.348 \pm 0.110$  compared to movement on the  $\mu\text{SG}_L$ ; however, this difference was not statistically significant ( $p = 0.47$ ). These values are in accordance with previously reported TI values of approximately 0.25 for vascular smooth muscle cell migration on hydrogel-based rigidity gradients.<sup>11</sup>

The speed of cell movement was also found to be affected by the micropost array gradients during the 18 hour studies. Specifically, cell speeds were observed to vary with respect to the direction of the mechanical stimuli. For migration in the direction of increasing micropost stiffness, BAECs on the  $\mu\text{SG}_L$  and  $\mu\text{SG}_H$  exhibited average speeds of  $7.5 \pm 0.5 \mu\text{m h}^{-1}$  and  $7.0 \pm 0.7 \mu\text{m h}^{-1}$ , respectively. For movement opposite to the direction of increasing stiffness, the average speed of BAEC migration on the  $\mu\text{SG}_L$  decreased to  $6.6 \pm 0.5 \mu\text{m h}^{-1}$ ; however, this difference was not statistically significant ( $p = 0.24$ ). In contrast, the average speed of BAEC migration on the  $\mu\text{SG}_H$  decreased significantly to  $4.8 \pm 0.6 \mu\text{m h}^{-1}$  for movement opposite to the direction of increasing stiffness ( $p < 0.05$ ). As prior work has not yet elucidated the effects of rigidity gradients on the directional speed of cell movement, these results suggest that further study is needed to examine cell speeds in response to unidirectional substrate stiffness cues.

Although the cellular response to the microtopographic mechanical stimuli was found to be consistent with durotaxis predictions and prior work, the experimental results cannot be attributed exclusively to cellular durotaxis for the current study. In this work, the spacing surrounding individual microposts was modulated to ensure that the overall %ECM and topographic surface area remained constant over both microtopographic substrates; however, it remains unclear how increasing the micropost-specific top surface area in the absence of gradients in %ECM or topographic density might affect cell motility. Thus, future applications of this technique for studying the durotaxis phenomenon specifically should employ microposts with uniform top surface areas (e.g., via gradients of elliptical microposts).

## Conclusions

Micropost array gradients provide an effective technique for engineering the mechanical properties of discrete, microscale substrate features via simple, accurate, and repeatable fabrication processes. Here, unidirectional micropost array stiffness gradients were employed to investigate cell motility in response to microtopographic mechanical cues. BAECs seeded on the micropost array gradients exhibited higher displacements and speeds in the direction of increasing micropost stiffness versus opposite to that direction. Additionally, higher gradient strength was found to enhance this directional response. A TI applied to quantify the migratory results revealed that cell movement was biased in the direction of the substrate-based mechanical stimuli. These results suggest that the methodology for fabricating micropost array stiffness gradients may offer a unique and passive method to regulate the motile processes of

seeded cells. The rigidity of the substrate has been demonstrated to affect a variety of cells, which suggests the current technique can be adapted to examine how additional cell types respond to microtopographic stiffness gradients. As prior works have used micropost arrays to measure cellular forces on the substrate, the current methodology could be employed to elucidate the effects of mechanical gradients on the traction forces of motile cells. Here, substrates were designed with post-to-post differences in stiffness of  $0.5 \text{ nN } \mu\text{m}^{-1}$  and  $7.5 \text{ nN } \mu\text{m}^{-1}$ ; however, the gradient strength of the micropost arrays can be tailored corresponding to specific applications. Although this study employed unidirectional micropost array gradients in a linear arrangement, individual microposts can be independently placed and geometrically tuned to achieve diverse configurations of substrate stiffness (e.g., radial gradients). As a method for investigating the cellular response to substrate stiffness cues, micropost array gradients offer a simple, yet powerful technique for applying unidirectional mechanical stimuli to living cells.

## Notes and references

- 1 G. C. Gurtner, S. Werner, Y. Barrandon and M. T. Longaker, *Nature*, 2008, **453**, 314–321.
- 2 R. J. Petrie, A. D. Doyle and K. M. Yamada, *Nat. Rev. Mol. Cell Biol.*, 2009, **10**, 538–549.
- 3 A. M. Kloxin, A. M. Kasko, C. N. Salinas and K. S. Anseth, *Science*, 2009, **324**, 59–63.
- 4 M. E. Chicurel, R. H. Singer, C. J. Meyer and D. E. Ingber, *Nature*, 1998, **392**, 730–733.
- 5 C. G. Galbraith, K. M. Yamada and M. P. Sheetz, *J. Cell Biol.*, 2002, **159**, 695–705.
- 6 C.-M. Lo, H.-B. Wang, M. Dembo and Y.-L. Wang, *Biophys. J.*, 2000, **79**, 144–152.
- 7 A. J. Engler, S. Sen, H. L. Sweeney and D. E. Discher, *Cell*, 2006, **126**, 677–689.
- 8 J. P. Fu, Y. K. Wang, M. T. Yang, R. A. Desai, X. A. Yu, Z. J. Liu and C. S. Chen, *Nat. Methods*, 2010, **7**, 733–795.
- 9 D. S. Gray, J. Tien and C. S. Chen, *J. Biomed. Mater. Res., Part A*, 2003, **66**, 605–614.
- 10 A. Kidoaki and T. Matsuda, *J. Biotechnol.*, 2008, **133**, 225–230.
- 11 B. C. Isenberg, P. A. DiMilla, M. Walker, S. Kim and J. Y. Wong, *Biophys. J.*, 2009, **97**, 1313–1322.
- 12 J. Y. Wong, A. Velasco, P. Rajagopalan and Q. Pham, *Langmuir*, 2003, **19**, 1908–1913.
- 13 A. Saez, M. Ghibaudo, A. Buguin, P. Silberzan and B. Ladoux, *Proc. Natl. Acad. Sci. U. S. A.*, 2007, **104**, 8281–8286.
- 14 N. J. Sniadecki and C. S. Chen, in *Methods in Cell Biology—Cell Mechanics*, 2007, vol. 83, pp. 313–328.
- 15 J. L. Tan, J. Tien, D. M. Pirone, D. S. Gray, K. Bhadriraju and C. S. Chen, *Proc. Natl. Acad. Sci. U. S. A.*, 2003, **100**, 1484–1489.
- 16 I. K. Lin, Y.-M. Liao, Y. Liu, K.-S. Ou, K.-S. Chen and X. Zhang, *Appl. Phys. Lett.*, 2008, **93**, 251907.
- 17 S. Hsu, R. Thakar, D. Liepmann and S. Li, *Biochem. Biophys. Res. Commun.*, 2005, **337**, 401–409.
- 18 D. H. Kim, C. H. Seo, K. Han, K. W. Kwon, A. Levchenko and K. Y. Suh, *Adv. Funct. Mater.*, 2009, **19**, 1579–1586.
- 19 D.-H. Kim, K. Han, K. Gupta, K. W. Kwon, K.-Y. Suh and A. Levchenko, *Biomaterials*, 2009, **30**, 5433–5444.
- 20 M. McCutcheon, *Physiol. Rev.*, 1946, **26**, 319–336.